



Title	The elution profile of immobilized liposome chromatography: determination of association and dissociation rate constants.
Author(s)	Ohno, Masako; Ikehara, Tatsuya; Nara, Toshifumi; Kamo, Naoki; Miyauchi, Seiji
Citation	Biochimica et Biophysica Acta (BBA) - Biomembranes, 1665(1-2), 167-176 <a href="https://doi.org/10.1016/j.bbamem.2004.07.007">https://doi.org/10.1016/j.bbamem.2004.07.007</a>
Issue Date	2004-10-11
Doc URL	<a href="http://hdl.handle.net/2115/16003">http://hdl.handle.net/2115/16003</a>
Type	article (author version)
File Information	BBAB1665-1-2.pdf



[Instructions for use](#)

**The Elution Profile of Immobilized Liposome Chromatography:  
Determination of Association and Dissociation Rate Constants**

Masako Ohno, Tatsuya Ikehara, Toshifumi Nara, Naoki Kamo\*  
and  
Seiji Miyauchi\*

Laboratory of Biophysical Chemistry, Graduate School of  
Pharmaceutical Sciences, Hokkaido University, Sapporo  
060-0812, Japan

**Address correspondence to:** S. Miyauchi, Tel,  
+81-11-706-3936; Fax, +81-11-706-4984; E-mail,  
[miyamiya@tc5.so-net.ne.jp](mailto:miyamiya@tc5.so-net.ne.jp), or N. Kamo, Tel,  
+81-11-706-3923; Fax, +81-11-706-4989; E-mail,  
[nkamo@pharm.hokudai.ac.jp](mailto:nkamo@pharm.hokudai.ac.jp)

**[Running title]** Elution profile of ILC

**[Key words]** plate height, phosphonium cation, retention time,  
band-broadening, rate constant

### Abstract

The interaction of lipophilic cations, tetraphenylphosphonium and triphenylphosphonium homologues with liposomes was investigated using immobilized liposome chromatography (ILC). Large unilamellar liposomes with a mean diameter of 100 nm were stably immobilized in chromatographic gel beads by avidin-biotin. The distribution coefficient calculated from  $(V_e - V_0)/V_s$  ( $V_e$ , retention volume;  $V_0$ , the void volume;  $V_s$ , the stationary phase volume) and was found to be independent of flow rate, injection amount and gel bed volume, which is consistent with chromatograph theory. The relationship between the bandwidth and solvent flow rate did not follow band-broadening theories reported thus far. We hypothesized that the solvent might be forced to produce large eddies, spirals or turbulent flow due to the presence of liposomes fixed in the gel. Therefore, we developed a new theory for ILC elution: The column is composed of a number of thin disks containing liposomes and solution, and within each disk the solution is well-mixed. This theory accounts for our results, and we were able to use it to estimate the rate constants of association and dissociation of the phosphonium to/from liposomes.

## Introduction

Column chromatography or high-performance liquid chromatograph (HPLC) is a powerful method used for materials separation and analysis [ex. 1]. This method has been used to investigate the interaction of biological materials with their host molecules [reviews, 1-6]. Estimation of the binding constants of membrane proteins with their ligands can be carried out by "quantitative affinity chromatography" or IBAC (immobilized biomembrane affinity chromatography) [3,4], in which membrane protein immobilization on the stationary phase is indispensable. One type of IBAC involves the use of IAM (immobilized artificial membrane stationary phase) [4,6], and others use immobilized liposomes, proteoliposomes (membrane proteins embedded in liposomes), or membrane vesicles or intact cells trapped in a gel [3,7-9]. Recently, several methods were developed to permit the immobilization of these materials[10]. In particular, an avidin-biotin binding permits the high-yield stable immobilization of liposomes [11]. The interactions of drugs with lipid membranes have been investigated using liposome-immobilized columns [12] and it was found that this method, called immobilized liposome chromatography (ILC) [13], yields more accurate binding constants than the conventional methods even if the interactions are weak [12,14].

Using ILC, we determined the interaction of the

lipophilic cations tetraphenylphosphonium ( $\text{TPP}^+$ ) and triphenylphosphonium homologues  $(\text{Phe})_3\text{-P}^+(\text{CH}_2)_n\text{CH}_3$ ,  $n = 0-5$ ; see Table 1) with liposomes (lipid bilayers). These phosphonium cations can efficiently penetrate the membrane. Some of them, tetraphenyl phosphonium and triphenyl methyl phosphonium are used extensively to estimate the membrane potential of cells, organelles and vesicles, which are too small for microelectrodes to be impaled [15]. Here we used these derivatives as the model compounds, which interact with liposomes. The membrane distribution coefficients of these cations were determined from the retention volume or retention time [1]. We analyzed the width of the elution band (variance) and found that previous theories on HPLC band broadening did not adequately explain the results. The reasons for the discrepancies were attributed to the presence of liposomes, and disorderly solvent flow. Therefore, for ILC, a new mathematical model was developed, whereby the column consists of a number of disks (thin zones) connected in series containing liposomes, and each disk is assumed to be well mixed because of turbulent flow of the elution solvents caused by the liposomes. Thus, each disk (zone) was treated as a "well-mixed zone". This new ILC theory (named as a Mixing-Zone Model) accounts for obtained experimental data and allowed us to estimate the association and dissociation rate constants of the above-mentioned lipophilic ions to/from liposomes as well as the distribution

coefficient.

## Materials and Methods

### **Materials**

Sephacryl S-1000 (sephacryl) was purchased from Amersham Pharmacia Biotech (Uppsala, Sweden), and triphenylmethyl-phosphonium (TPMP<sup>+</sup>), triphenylethyl-phosphonium (TPEP<sup>+</sup>), triphenylpropyl-phosphonium (TPPP<sup>+</sup>), triphenylbutyl-phosphonium (TPBP<sup>+</sup>), triphenylamyl-phosphonium (TPAP<sup>+</sup>), triphenylhexyl-phosphonium (TPHP<sup>+</sup>), and tetraphenyl-phosphonium (TPP<sup>+</sup>) were purchased from Tokyo Kasei (Tokyo, Japan). The chemical structures of these phosphonium cations are shown in Table 1. Egg white avidin was purchased from Calbiochem (La Jolla, CA), and egg yolk phosphatidylcholine (EPC > 99%) and biotin-cPE (1,2 dioleoylphosphatidyl-ethanolamine-N-(cap biotinyl)) were obtained from Avanti Polar Lipids (Alabaster, AL). N-2-hydroxyethylpiperazine-N'-2-ethane-sulfonic acid (HEPES) was acquired from Dojindo Laboratories (Kumamoto, Japan), and 4-nitrophenylchloroformate was obtained from Aldrich (Milwaukee, WI). All other chemicals used were of the highest purity available.

### **Avidin-gel coupling**

Sephacryl gel was activated by 4-nitrophenyl chloroformate with a chloroformate density of 20 - 30  $\mu\text{mol/mL}$  gel, and avidin was coupled to the activated gel at 3 mg/mL gel [11]. The activated gel was washed in water, 0.2 M acetic acid and 10 mM NaOH (100 mL each for 1 g gel) for three cycles on a 10  $\mu\text{m}$  filter (Millipore, Bedford, MA) fixed in a glass funnel. The avidin-gel was stored at 4 °C in buffer H (10 mM HEPES and 150 mM NaCl at pH 7.4) supplemented with 3 mM  $\text{NaN}_3$ .

#### ***Preparation and immobilization of biotinylated liposomes***

Large unilamellar liposomes (LUVs) were prepared by extrusion as previously described [11], and were composed of EPC supplemented with 2 mol % of biotin-cPE. The mean diameter was  $100 \pm 20$  nm as analyzed by dynamic light scattering. For immobilization, biotinylated liposomes were mixed with avidin-Sephacryl under nitrogen for 2-3 hr at 23 °C or overnight. Non-immobilized liposomes were removed by washing with buffer H on a 10  $\mu\text{m}$  filter. The amounts of phospholipids immobilized as liposomes in the gel beads were determined using the method of Bartlett [16].

#### ***Immobilized liposome chromatography (ILC)***

Gel beads containing avidin-biotin immobilized liposomes were packed into a 5 mm I.D. x 5 cm gel bed in a glass column (HR 5/5, Pharmacia Biotech, Uppsala, Sweden), and the

liposome column was placed in a column oven (L7300, Hitachi, Tokyo, Japan). Chromatographic runs were performed using a Hitachi inert-type HPLC system equipped with an injector connected to a HPLC pump (L7120, Hitachi, Tokyo, Japan) and a microcomputer interfaced UV detector (L4200, Hitachi, Tokyo, Japan). Lipophilic cations were applied to the immobilized-liposome gel bed and eluted with buffer H at 0.3 - 1.5 mL/min. The loss of lipid from the gel was 3 - 5 % after 5 months storage at 4 °C. Stability in the present ILC was demonstrated by the fact that only 7 % of the liposomes was lost after 60 runs at different temperatures (from 10 to 40 °C). [11, 12]

### **Data analysis**

The elution patterns were analyzed by the moment analysis. The first moment of the elution time distribution represented the retention time (or mean resident time), and the second moment, of the mean of the distribution, represented the variance in the elution profile [17]. The retention time ( $\bar{t}$ ) and variance of the elution profiles were calculated from the following equations:

$$\bar{t} = \frac{\int_0^{\infty} t \cdot C(t) dt}{\int_0^{\infty} C(t) dt} \quad (1)$$



$$\text{variance} = \frac{\int_0^{\infty} (t - \bar{t})^2 \cdot C(t) dt}{\int_0^{\infty} C(t) dt} \quad (2)$$

where  $C(t)$  represents the concentration of the solute in the eluant at time  $t$ . The time was corrected by the dead-time (breakthrough time). The retention volume ( $V_e$ ) was estimated by multiplying  $\bar{t}$  by the flow rate ( $Q$ ), and the distribution coefficient for lipophilic cations between stationary liposomes and the aqueous phase,  $K_{LM}$ , was calculated by the equation [1,18]:

$$K_{LM} = \frac{V_e - V_0}{V_s} \quad (3)$$

Here,  $V_0$  is the void volume, which is estimated by multiplying  $Q$  and  $t_0$  associated with a small hydrophilic molecule such  $N_3^-$  that does not interact with the liposomes, and  $V_s$  is the stationary phase volume (see below).

Since the volume per phospholipid molecule packed into the liposome membrane is well-documented [19],  $V_s$  can be calculated from the amount of EPC: When a quantity of immobilized liposomes  $A$  has units of mmol,  $V_s$ (mL) is related to  $A$  by  $V_s = 0.755 \cdot A$  (4)

provided that the outer and inner leaflets of the unilamellar liposomal membranes are accessible to the solute [14]. The combination of Eqs. 3 and 4 yields:

$$K_{LM} = \frac{V_e - V_0}{0.755 \cdot A} \quad (5)$$

The theory developed here fulfills the chromatographic equations, Eq. 3 and Eq. 5, which are independent of the flow rate of the eluant.

### ***Models used in data analysis***

The position and broadening of the elution band is theoretically analyzed to elucidate what factors determine these quantities. Two extreme models, (A) the diffusion-reaction-transport model and (B) the well mixed zone model are used in this study. The former model is a conventional and simple model that analysis molecules are assumed to move through ILC without axial diffusion. By contrast, the latter model is a new model developed in this study that the zonal well-mixing is assumed and this mixing zone moves down by the column flow.

#### ***(A) The diffusion-reaction-transport***

We will consider that a cylindrical column packed with immobilized liposome resins. Let  $x$  be a distance from the bottom of the column so that  $x = 0$  is the bottom of the column and  $x = h$  is the top of the column. At time  $t = 0$ , the molecule to be analyzed is introduced at the top of column, with the axis of the column oriented along the direction of the column flow. Molecules move through the column by the column flow and diffusion. The movement of molecules is delay as a consequence of molecules interacting with liposome. Let  $V_0$  and  $V_s$  be the volumes of mobile and stationary phases, respectively. The cross-sectional areas of mobile and

stationary phases can be designated by  $A_0 = V_0/h$  and  $A_s = V_s/h$  respectively. On the basis of the mass conservation, this model gives the following partial differential equations [20]:

$$\left(\frac{\partial C}{\partial t}\right)_x \cdot A_0 = D\left(\frac{\partial^2 C}{\partial x^2}\right)_t \cdot A_0 + u\left(\frac{\partial C}{\partial x}\right)_t \cdot A_0 - k_1 C \cdot A_0 + k_{-1} L \cdot A_s \quad (6)$$

$$\left(\frac{\partial L}{\partial t}\right)_x = k_1 C \cdot A_0 - k_{-1} L \cdot A_s \quad (7)$$

Here,  $C$  = the solute concentration in the mobile phase at  $x$ ,  $t$ ;  $A_0$  = cross sectional area of the void (solvent flow);  $D$  = diffusion coefficient of the solute along the axis  $x$ ;  $u$  = the velocity of the solvent flow in units of cm/s ( $Q$  in the text is equivalent to  $uA_0$ );  $L$  = solute concentration adsorbed by the liposome;  $A_s$  = cross sectional area of the liposome in the column. Here, we assume that the radial diffusion within the column is negligible.

Defining dimensionless reduced variables of  $p$  and  $q$  by

$$p = \frac{CA_0}{I}, q = \frac{LA_s}{I}, \text{ Eq. 6 and 7 are recast as:}$$

$$\frac{\partial p}{\partial t} = u \frac{\partial p}{\partial x} + D \frac{\partial^2 p}{\partial x^2} - k_1 p + k_2 q \quad (8)$$

$$\frac{\partial q}{\partial t} = k_1 p - k_{-1} q \quad (9)$$

Here,  $I$  represents the amount of solute injected on the top of the column at  $t = 0$ . Defining  $\Delta = ut + x - h$  and

$\rho = \frac{k_1 k_{-1}}{u^2} (h - x)$ , the solutions for Eq.8 and 9 are found with the initial condition of  $p(h, t) = 0$  using the Laplace transform as:

$$\begin{aligned} p(x, t) &= \exp[-k_1(h - u) / u] \left[ \delta(\Delta) + H(\Delta) \exp(-k_{-1}\Delta / u) \cdot \sqrt{\rho / \Delta} \cdot I_1(2\sqrt{\rho\Delta}) \right] \\ q(x, t) &= (k_1 / u) \exp[-k_1(h - x) / u] \cdot H(\Delta) \exp(-k_{-1}\Delta / u) \cdot I_0(2\sqrt{\rho\Delta}) \end{aligned}$$

where the function H is a Heaviside step function, and  $I_0$  and  $I_1$  are modified Bessel functions. From these equations, we obtained the mean resident time as:

$$\bar{t} = \lim_{\tilde{s} \rightarrow 0} \left( -\frac{d}{d\tilde{s}} \ln f_{C(0, t)}(\tilde{s}) \right) = \left( 1 + \frac{k_1}{k_{-1}} \right) \frac{h}{u} = \left( 1 + \frac{k_1}{k_{-1}} \right) \frac{V_0}{Q} \quad (10)$$

Here,  $f_{C(0, t)}(\tilde{s})$  represents the Laplace transformed equation of  $C(0, t)$  which is the solute concentration at the outlet of the column at time  $t$ . Note that  $hA_0 = V_0$  and  $uA_0 = Q$ . According to the standard notation for HPLC, we define the retention factor as  $k = \frac{\bar{t} - t_0}{t_0}$  [1] where  $t_0$  stands for the dead time

(breakthrough time [1]) or retention time of an un-retained solute. The value of  $t_0$  is calculated from Eq.10 with  $k_1 = 0$ , so that  $k$  value is:

$$k = \frac{\bar{t} - t_0}{t_0} = \frac{k_1}{k_{-1}} \quad (11)$$

Furthermore,  $k$  is related to the distribution coefficient,  $K_{LM}$  as [1]:

$$k = K_{LM} \frac{V_s}{V_0} \quad (12)$$

From Eq. 10, 11 and 12, therefore, we obtain:

$$\bar{t} = \left(1 + K_{LM} \frac{V_s}{V_0}\right) \frac{V_0}{Q} \quad (13)$$

Eq.13 is identical to Eq.3, because  $V_e = \bar{t} \cdot Q$ .

The variance is given as:

$$variance = \lim_{\tilde{s} \rightarrow 0} \left( -\frac{d^2}{d\tilde{s}^2} \ln f_{C(0,t)}(\tilde{s}) \right) = \frac{k_1}{k_{-1}^2} \cdot \frac{2h}{u} = \frac{2K_{LM}}{k_{-1}} \cdot \frac{V_s}{Q} \quad (14)$$

#### **(B) Well-mixed zone model**

As shown below, Eq. 14 does not fold for the present experimental results. Hence, we develop a new theory for ILC as follows: In the ILC column, we used the gel-iffiltration resin as a supporting material for liposome immobilization. On the molecular scale, the interior of the column can be thought as a network of tortuous channels of various sizes, since the resin has a large number of pores, and consists of large as well as tortuous channels and caves. Liposomes are immobilized along tortuous channels and caves. This geographical property causes the well-mixing zone of the solutes with significant thickness, even if there is no interaction with liposome. Therefore, to develop a new mathematical analysis, let the whole column divided into the number N of disks (zones), where the molecules are well mixed (Fig.1). The molecules are sequentially moved down from the

$i$ -th zone to the  $(i+1)$ -th zone on a stream of solvent. The following mass-balance equation holds true for the  $i$ -th disk (zone):

For the mobile phase,

$$\begin{aligned} \frac{V_0}{N} \frac{dC_1}{dt} &= -(Q + \frac{k_1 V_0}{N}) C_1 + \frac{k_{-1} V_s}{N} C_{1,s} \quad (\text{for } i = 1) \\ \frac{V_0}{N} \frac{dC_i}{dt} &= -(Q + \frac{k_1 V_0}{N}) C_i + \frac{k_{-1} V_s}{N} C_{i,s} + Q C_{i-1} \quad (\text{for } i = 2 \sim N) \end{aligned} \quad (15)$$

Here, the first term  $(-QC_i)$  and last term  $(QC_{i-1})$  represent the amount of solute flowing out to the lower disk (zone) and the amount entering from the upper disk (zone), respectively due to solvent flow whose flow rate is  $Q$ .

For the stationary phase,

$$\frac{V_s}{N} \frac{dC_{i,s}}{dt} = -\frac{k_{-1} V_s}{N} C_{i,s} + \frac{k_1 V_0}{N} C_i \quad (\text{for } i = 1 \sim N) \quad (16)$$

where the notations  $k_1$  and  $k_{-1}$  are the same as in Eq. 10 and 14;  $\frac{V_0}{N}$  and  $\frac{V_s}{N}$  are the volumes of the solution and stationary phase in each disk, respectively; and  $C_i$  and  $C_{i,s}$  are the solute concentrations of the mobile and stationary phases in the  $i$ -th disk, respectively. The initial conditions are:

$$C_1 = \text{constant} = C(0), \quad C_i = 0 \quad \text{and} \quad C_{i,s} = 0$$

where  $C(0)$  is equal to the amount of solute injected at  $t=0$  divided by the volume of the first disk ( $V_0/N$ ). For the first disk (the upper-most disk in the column), the solute is

instantaneously mixed to give a concentration of  $C(0)$  within the disk. The  $2N$  differential equations of Eq. 15 and 16 are Laplace-transformed to obtain  $2N$  simultaneous linear equations, from which  $C_N$  is solved if the concentration of outflow from the  $N$ -th disk is monitored. First, consider the  $i$ -th disk: The Laplace transformation of Eq.15 and 16 gives:

$$\frac{V_0}{N} \tilde{s} f_i(\tilde{s}) = -\left(Q + k_1 \frac{V_0}{N}\right) f_i(\tilde{s}) + \frac{k_{-1} V_s}{N} g_i(\tilde{s}) + Q f_{i-1}(\tilde{s}) \quad (17)$$

$$\frac{V_s}{N} \tilde{s} g_i(\tilde{s}) = -\frac{k_{-1} V_s}{N} g_i(\tilde{s}) + \frac{k_1 V_0}{N} f_i(\tilde{s}) \quad (18)$$

where  $f_i(\tilde{s})$  and  $g_i(\tilde{s})$  are the Laplace transformed functions of  $C_i$  and  $C_{i,s}$ , respectively. Elimination of  $g_i(\tilde{s})$  from these equations gives:

$$f_i(\tilde{s}) = \frac{\tilde{s} + k_{-1}}{\tilde{s}^2 + \left(k_1 + k_{-1} + \frac{Q}{V_N}\right)\tilde{s} + k_{-1} \frac{Q}{V_N}} \cdot \frac{Q}{V_N} \cdot f_{i-1}(\tilde{s})$$

Here,  $V_N = \frac{V_0}{N}$ .

This equation leads to the relationship:

$$f_N(\tilde{s}) = \frac{(\tilde{s} + k_{-1})^{N-1}}{\left\{ \tilde{s}^2 + \left(k_1 + k_{-1} + \frac{Q}{V_N}\right)\tilde{s} + k_{-1} \frac{Q}{V_N} \right\}^{N-1}} \cdot \left(\frac{Q}{V_N}\right)^{N-1} \cdot f_1(\tilde{s}) \quad (19)$$

which implies the necessity of the  $f_1(\tilde{s})$  expression.

For the first disk, the Laplace transformation of Eq.15 and 16 gives:

$$\frac{V_0}{N} [\tilde{s}f_1(\tilde{s}) - c(0)] = -\left(Q + k_1 \frac{V_0}{N}\right)f_1(\tilde{s}) + \frac{k_{-1}V_s}{N} g_1(\tilde{s}) \quad (20)$$

$$\frac{V_s}{N} \tilde{s}g_1(\tilde{s}) = -\frac{k_{-1}V_s}{N} g_1(\tilde{s}) + \frac{k_1V_0}{N} f_1(\tilde{s}) \quad (21)$$

Elimination of  $g_1(\tilde{s})$  from Eq.20 and 21 yields:

$$f_1(\tilde{s}) = \frac{\tilde{s} + k_{-1}}{\tilde{s}^2 + \left(k_1 + k_{-1} + \frac{Q}{V_N}\right)\tilde{s} + k_{-1} \frac{Q}{V_N}} c(0) \quad (22)$$

Insertion of Eq.22 into Eq.19 produces  $f_N(\tilde{s})$ , which is the Laplace-transformed equation for  $C_N$ .

$$f_N(\tilde{s}) = \frac{(\tilde{s} + k_{-1})^N \left(\frac{Q}{V_N}\right)^{N-1} c(0)}{\left\{ \tilde{s}^2 + \left(k_1 + k_{-1} + \frac{Q}{V_N}\right)\tilde{s} + k_{-1} \frac{Q}{V_N} \right\}^N} \quad (23)$$

where  $V_N$  represents  $V_0/N$ . From Eq. 23, the mean resident time and variance can be calculated as:

$$\bar{t} = \lim_{\tilde{s} \rightarrow 0} \left( -\frac{d}{d\tilde{s}} \ln f_N(\tilde{s}) \right) = N \left( 1 + \frac{k_1}{k_{-1}} \right) \frac{V_N}{Q} = \left( 1 + K_{LM} \frac{V_s}{V_0} \right) \frac{V_0}{Q} \quad (24)$$

$$\begin{aligned} \text{variance} &= \lim_{\tilde{s} \rightarrow 0} \left( -\frac{d^2}{d\tilde{s}^2} \ln f_N(\tilde{s}) \right) = \frac{k_1}{k_{-1}^2} \cdot \frac{2}{Q} + \frac{1}{N} \left( 1 + \frac{k_1}{k_{-1}} \right)^2 \left( \frac{V_0}{Q} \right)^2 \\ &= \frac{K_{LM}}{k_{-1}} \cdot \frac{V_s}{V_0} \cdot \frac{2}{Q} + \frac{1}{N} \left( 1 + K_{LM} \frac{V_0}{V_s} \right)^2 \left( \frac{V_0}{Q} \right)^2 \end{aligned} \quad (25)$$



## **Results and Discussion**

### **Retention time (mean resident time, $\bar{t}$ ) analysis**

Figure 2 shows the elution profiles of a typical lipophilic cation TPP<sup>+</sup> from ILC column for elution flow rates Q of 0.3 - 1.5 ml/min. For decreasing the flow rate, the retention time increases along with the bandwidth. We first consider the retention time (mean resident time,  $\bar{t}$ ) calculated from Eq.1. The  $\bar{t}$  values of various lipophilic cations are plotted against the reciprocal of the flow rate in Fig. 3, which yielded straight lines with different slopes for the respective lipophilic phosphonium cations. The chemical structures and respective n-values of the phosphonium cations used are listed in Table 1.

A chromatography column should consist of a mobile and stationary phase. The initial condition can be mathematically expressed by the Dirac delta function: The solute is first introduced at the top of column, and its concentration is distributed in an infinitesimally thin layer. Solutes are assumed to move down the column by elution without the turbulence, which is referred to as diffusion-reaction-transport. This activity can be described as follows [20]:

$$\begin{aligned}\bar{t} &= \frac{V_e}{Q} = \left(1 + \frac{k_1}{k_{-1}}\right) \frac{V_0}{Q} \\ &= \left(1 + K_{LM} \cdot \frac{V_s}{V_0}\right) \frac{V_0}{Q}\end{aligned}\tag{13}$$

Here,  $k_1$  and  $k_{-1}$  represent the rate constants for association and dissociation between the solute and stationary phase, respectively, and  $K_{LM}$  is given by Eq.3 (see also Eq.11 and 12, and  $V_e = \bar{t} \cdot Q$ ). The results in Fig. 3 follow Eq.13, which describes the proportionality of  $\bar{t}$  against the reciprocal of the flow rate,  $1/Q$ .

Eq.13 shows that  $K_{LM}$  values are independent of the flow rate, total solute mass and gel bed volume. Figure 4 shows good agreements between this theory and the experimental results.

#### ***Analysis of elution profile variance***

We next consider the bandwidth or variance of the elution peak. The diffusion-reaction-transport model mentioned above can be described by the relationship:

$$variance = \frac{2K_{LM}}{k_{-1}} \cdot \frac{V_s}{Q} \quad (14)$$

Although this equation predicts a decrease in variance with an increasing  $Q$ , it does not quantitatively explain the data shown in Fig. 5: Here, the variance is plotted against  $1/Q$ , indicating that the lines are not straight but quadratic. This implies that the simple diffusion-reaction-transport model is invalid.

#### ***Sequential mixing zone model: A new theory for band broadening in ILC***

The variance of the azide elution pattern also exhibits a parabolic increase in the plot of variance against  $1/Q$  (data not shown). Azide anion is hydrophilic and little interaction with hydrophobic liposomes occurs. Hence, this discrepancy is not caused by solute interaction with liposomes. On a molecular scale, the interior of a bed can be thought as a network of tortuous channels along which liposomes (100 nm in diameter) are immobilized. A schematic illustration of steric entrapment is given by Lee and Angilar [21]. This situation prevents zonal solute flow as simple diffusion-reaction-transport theory assumes, but large eddies or spiral flow might occur. Thus, a new theory to explain this is necessary. To develop a new mathematical analysis, we make the following assumptions (see Materials and Methods): the column is divided into a number of disks (zone) in which the solute is well mixed due to eddy flow of the solution caused by the liposomes. Note that *eddy flow* used in the present article is different from *eddy diffusion* used in HPLC theory [1,17]. The solutes are sequentially moved from the  $i$ -th disk to the  $(i+1)$ -th disk on a stream of solvent. We call this the well-mixed zone model. A similar concept is extensively used in chemical engineering, particularly when describing mixing in a chemical reactor [22]. In the field of the liver physiology, such a model is also used to describe the behavior of a compound and its metabolites [23,24]. According to this well-mixed zone model

(see Materials and Methods), the mean resident time and variance can be calculated as:

$$\bar{t} = N \left( 1 + \frac{k_1}{k_{-1}} \right) \frac{V_N}{Q} = \left( 1 + K_{LM} \frac{V_s}{V_0} \right) \frac{V_0}{Q} \quad (24)$$

$$\begin{aligned} \text{variance} &= \frac{k_1}{k_{-1}^2} \cdot \frac{2}{Q} + \frac{1}{N} \left( 1 + \frac{k_1}{k_{-1}} \right)^2 \left( \frac{V_0}{Q} \right)^2 \\ &= \frac{K_{LM}}{k_{-1}} \cdot \frac{V_s}{V_0} \cdot \frac{2}{Q} + \frac{1}{N} \left( 1 + K_{LM} \frac{V_0}{V_s} \right)^2 \left( \frac{V_0}{Q} \right)^2 \end{aligned} \quad (25)$$

Eq. 24 is the same as the retention time (mean resident time) derived from the diffusion-reaction-transport scheme described above (Eq.13). Therefore, with this model the equilibrium constant can be estimated using the chromatography equation (Eq.3). Eq.25 can be used to explain the experimental parabolic relationship between variance and  $1/Q$  as shown in Fig. 5. Using a nonlinear iterative least square method, the values of  $k_1$ ,  $k_{-1}$  and  $N$  can be determined. The estimated values for the rate constants ( $k_1$ ,  $k_{-1}$ ) were  $10^2 \text{ sec}^{-1}$ , which are consistent with those previously reported [25,26]. The estimated values of  $N$  were 40 ~ 50 (see below).

The estimation of  $N$  as a function of the injection and column volumes may be used to describe its physical meaning. It is feasible that the injection solution directly enters the top of the column and is instantaneously distributed in the upper-most disk (zone). Due to solvent streaming, the solution in this disk moves down to a new adjacent disk.

Therefore, we assume as a first approximation that for the number of the well-mixed disks (zones),  $N$  may be obtained by dividing the mobile phase volume by the injection volume; for a 1 mL column and 20  $\mu$ L injection volume, the number  $N$  is 50. As shown in Fig. 6,  $N$  decreases for increasing injection volume. When two columns prepared by the same procedure were connected in series (equivalent to double the column length),  $N$  increased two-fold (data not shown). As shown in Fig. 6,  $N$  depends on the injection volume, but is not exactly proportional to its inverse. Thus,  $N$  is not simply governed by the geometrical factors, but is an adjustable parameter. If the value of  $N$  is governed by the geometrical factors, the  $N$  value would be estimated by dividing the volume of the column by that of the solute injection. However, the  $N$  value showed a little difference from that estimated by the geometrical parameters. According to this model, it is likely that the  $N$  value is affected by the extent of mixing in the ILC column. The estimation of  $N$  value will be influenced when the extent of the well-mixing is varied with the analyzed solute, lipid amount and lipid type *etc.* Thus, a future problem is how these factors affect the value of  $N$ . We do not know at present that if determined values of  $N$  would contain some errors, how this error varies the estimated values of  $k_1$  and  $k_{-1}$ , although the estimated rate constants ( $k_1$  and  $k_{-1}$ ) remained unchanged irrespective of the injection

volume (see Fig. 7) that changes the value of  $N$ . To clarify this effect will be done by the simulation study on the effect of varying  $N$  on the estimation of the  $k_1$  and  $k_{-1}$  values.

The association ( $k_1$ ) and dissociation ( $k_{-1}$ ) rate constants of various phosphonium analogues are depicted in Fig. 8. The rate constants for compounds with an even number of hydrocarbon chains (even  $n$ ) are larger than those with odd number. This zigzag pattern with respect to  $n$  is previously called the 'even-odd pattern' [27]. On the other hand, the equilibrium distribution coefficients,  $K_{LM}$ , increase smoothly when the number of carbon atoms in the chain increases [14,28], since  $K_{LM} = \frac{k_1}{k_{-1}} \frac{V_0}{V_s}$  (see Eq. 11 and 12) eliminates the 'even-odd pattern'.

The even-odd pattern for phosphonium cations occurs for various phenomena: it was first observed for the activation energy of permeation through a phospholipid bilayer reported by Ono et al [27]. They also reported that the bromide salts of phosphonium cations with odd patterns are less soluble in water than those with even  $n$ , and that the chemical shift of  $^{31}\text{P}$  exhibits a zigzag pattern. A similar zigzag pattern was observed for the partial molar volume and electric conductivity in water [14]. These observations suggest that the interaction of phosphonium cations with water differs depending on even or odd hydrocarbon chain length,  $n$ , which in turn, changes the rate constants  $k_1$  and  $k_{-1}$ . During

association to liposomes, phosphonium ions may be dehydrated while during dissociation they may be hydrated. The interaction of phosphonium ions with water may influence the speed of hydration and dehydration, resulting in the zigzag pattern for the rate constants as shown in Fig. 8. In addition, the dissociation rate constant seen in Fig. 8 increases with increasing  $n$ : highly hydrophobic ions are rapidly removed from the hydrophobic lipid layer. The molecular explanation for this observation is unclear. If phosphonium cations diffuse from the surface to the inner half-leaflet of liposomes, the greater value of  $k_{-1}$  for hydrophobic ions might be reasonable. Another possible mechanism is that larger molecules may be more rapidly squeezed out of lipid bilayer membranes. Although the dissociation rate constants ( $K_{-1}$ ) are larger for more hydrophobic ions, the values of  $K_{LM}$  are larger for these more hydrophobic ions since the increase in their association rate constants,  $k_1$ , is larger than that for  $k_{-1}$ .

***Comparison of the present theory with previous band-broadening HPLC theories***

In HPLC, band-broadening arises as a result of factors such as eddy diffusion, flow distribution, solute diffusion in the mobile phase and mass transfer between the stagnant mobile and stationary phases [1,17]. The band-broadening effect was described by van Deemter et al. [29] and Grushka et al. [30] in the mathematical form:

$$H = \frac{L \cdot (\text{variance})}{\bar{t}^2} = A + \frac{B}{Q} + (R_m + R_s)Q \quad (26)$$

where H = HETP (height equivalent to one theoretical plate); L = column length; A and B = constants;  $R_m$  = resistance to mass transfer of the solute in the mobile phase; and  $R_s$  = resistance to mass transfer of the solute in the stationary phase. Eddy diffusion and mass transfer effects are coupled, so that another expression describing is H [17]:

$$H = \frac{B}{Q} + R_s Q + \frac{1}{\frac{1}{A} + \frac{1}{R_m Q}} \quad (27)$$

An alternative coupling expression has been proposed [31]:

$$H = A + \frac{B}{Q} + \frac{DRQ}{D + RQ} \quad (28)$$

Since  $\bar{t}$  is proportional to the reciprocal of Q, these equations (Eq.26, 27 and 28) give the following relationship for variance as a function of Q:

$$\text{variance} \propto \frac{A}{Q^2} + \frac{B}{Q^3} + \frac{R_m + R_s}{Q} \quad (26')$$

$$\text{variance} \propto \frac{B}{Q^3} + \frac{R_s}{Q} + \frac{1}{\frac{Q^2}{A} + \frac{Q}{R_m}} \quad (27')$$

$$\text{variance} \propto \frac{A}{Q^2} + \frac{B}{Q^3} + \frac{DR}{DQ + RQ^2} \quad (28')$$

These equations do not explain the observation that variance occurs as a parabolic curve with respect to  $1/Q$  (see Fig. 5). If Q is small, Eq.26', 27' and 28' can be approximated by  $B/Q^3$ , which does not explain the observations. If Q is large



enough, the  $1/Q^3$  term can be neglected, and these equations approximately express a parabola equation; for example, Eq.26 can be approximated as  $\frac{R_m + R_s}{Q} + \frac{A}{Q^2}$ . According to an analysis of van Deemter et al. [29], the constant A is proportional to the diameter of the packed stationary material, which should be the same irrespective of the solutes used. Thus, this relationship does not explain the observations shown in Fig. 5. An explanation for the ILC elution profile using the above-described HPLC theories is therefore not possible. Other forms of plate height equations have been suggested [32,33], but these also do not explain the present results.

In the ILC column, the gel filtration resin, Sephacryl S-1000 was used as a supporting material for liposome immobilization. The matrices of this resin are large enough to immobilize large unilamellar liposomes with a diameter of ca. 0.1  $\mu\text{m}$ . The resin has a large number of pores, and consists of large as well as tortuous channels and caves. This structure may promote the well-mixed solvent flow in the mobile phase, which was incorporated in the present analysis. On the other hand, this effect in HPLC should be minimized. The discrepancy of this mixing effect between ILC and HPLC accounts for the inability of the HPLC theories to explain the ILC elution profile.

### ***Concluding remarks***

We have developed a new theory that describes the broadening of the elution peak, which we named the "well-mixed zone theory". Using this theory, we were able to estimate the association and dissociation rate constants of various phosphonium cations with liposomes. Although the present theory is not applicable to ordinary HPLC analysis, it might be applicable to elution pattern analysis of a column of molecular imprinted polymeric materials [35-37] because solvent flow might not be laminar due to the presence of bulky polymer materials.

### **Nomenclature**

$C(0)$ , solute concentration of the first disk for injection at the top of the column

$C_i$ , solute concentration in the mobile phase in the  $i$ -th disk (see Eq.8)

$C_{i,s}$ , solute concentration in the liposome phase in the  $i$ -th disk (see Eq.9)

$f_i(\tilde{s})$ , Laplace transformed function of  $C_i$

$g_i(\tilde{s})$ , Laplace transformed function of  $C_{i,s}$

$H$ , height equivalent to one theoretical plate (see Eq.26)

$k$ , retention factor defined as  $k = \frac{\bar{t} - t_0}{t_0}$

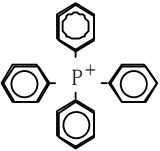
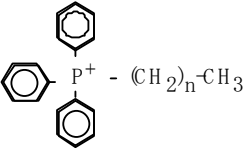
$k_1$ , association rate constant from the solution to the liposome (see Eq.8 and 9)  
 $k_{-1}$ , dissociation rate constant from the liposome to the solution  
 $K_{LM}$ , distribution coefficient in the immobilized liposome column defined as Eq.3 and Eq.12  
 $N$ , number of disks (zones) constituting the column. Within the each disk (zone), the mobile phase is assumed to be well-mixed (see Fig. 1)  
 $n$ , number of carbon atoms in the aliphatic hydrocarbon chain of each lipophilic phosphonium cation (see Table 1)  
 $Q$ , solvent flow rate  
 $\bar{t}$ , retention time calculated from Eq.1  
 $t_0$ , breakthrough time determined from the breakthrough time for  $N_3^-$ , which does not interact with liposomes  
 $\sigma$ , variance, quantity representing the bandwidth of the elution peak calculated from Eq.2  
 $V_e$ , retention volume calculated by  $\bar{t} \cdot Q$   
 $V_N$ ,  $V_0/N$ , the solution volume in each disk (zone)  
 $V_0$ , void volume determined from the breakthrough time of  $N_3^-$ , which does not interact with liposomes  
 $V_s$ , volume of the stationary liposome phase (see Eq.4)

### **Acknowledgement**

We thank Toshiyuki Kanamori of the Bio-nano Materials Team,

Research Center of Advanced Bionics, National Institute of Advanced Industrial Science and Technology (AIST) for his valuable discussion. This work was supported in part by a Grant-in-Aid for Scientific Research (KAKENHI) from the MEXT, Japan.

**Table 1. Lipophilic Phosphonium Cations Used in this Study**

Chemical Structure	Name	Abbreviations
	Tetraphenylphosphonium	TPP <sup>+</sup>
	Triphenyl- n=0, methylphosphonium n=1, ethylphosphonium n=2, propylphosphonium n=3, butylphosphonium n=4, amyolphosphonium n=5, hexylphosphonium	TPMP <sup>+</sup> TPEP <sup>+</sup> TPPP <sup>+</sup> TPBP <sup>+</sup> TPAP <sup>+</sup> TPHP <sup>+</sup>

## References

- [1] V.R. Meyer, Practical high-performance liquid chromatography (3<sup>rd</sup> edition), John Wiley and Sons, New York, 2000
- [2] D.S. Hage, High-performance affinity chromatography: a powerful tool for studying serum protein binding, J. Chromatogr. B 768 (2002) 3-30
- [3] I. Gottschalk, C. Lagerquist, S-S. Zuo, A. Lundqvist, P. Lundahl, Immobilized-biomembrane affinity chromatography for binding studies of membrane proteins, J. Chromatogr. B 768 (2002) 31-40
- [4] R. Moaddel, L. Lu, M. Baynham, I.W. Wainer, Immobilized receptor- and transporter-based liquid chromatographic phases for on-line pharmacological and biochemical studies: a mini-review, J. Chromatogr. B 768 (2002) 41-53
- [5] M. Markuszewski, R. Kaliszan, Quantitative structure-retention relationships in affinity high-performance liquid chromatography, J. Chromatogr. B 768 (2002) 55-66
- [6] A-F. Aubry, Applications of affinity chromatography to the study of drug-melanin binding interactions, J. Chromatogr. B 768 (2002) 67-74
- [7] P. Lundahl, Q. Yang, Liposome chromatography - liposomes immobilized in gel beads as a stationary phase for aqueous column chromatography, J. Chromatogr. 544

(1991)283-304

- [8] P. Lundahl, C.M. Zeng, C.L. Hagglund, I. Gottschalk, E. Greijer, J. Chromatogr. 722(1999)103-120
- [9] Q. Yang, X.Y. Liu, M. Hara, P. Lundahl, J. Miyake, Quantitative affinity chromatographic studies on mitochondrial cytochrome c binding to bacterial photosynthetic reaction center, reconstituted in liposome membranes and immobilized by detergent dialysis and avidin-biotin binding, Anal. Biochem. 280(2000)94-102
- [10] R.F. Taylor, Protein immobilization: Fundamentals and applications, Marcel Dekker, New York, 1991
- [11] Q. Yang, X.Y. Liu, S. Ajiki, M. Hara, P. Lundahl, J. Miyake, Avidin-biotin immobilization of unilamellar liposomes in gel beads for chromatographic analysis of drug-membrane partitioning, J. Chromatogr. B 707(1998)131-141
- [12] X.Y. Liu, Q. Yang, N. Kamo, J. Miyake, Effect of liposome type and membrane fluidity on drug-membrane partitioning analyzed by immobilized liposome chromatography, J. Chromatogr. A 913(2001)123-131
- [13] F. Beigi, Q. Yang, P. Lundahl, Immobilized-liposome chromatographic analysis of drug partitioning into lipid bilayers, J. Chromatogr. A 704 (1995) 315-321
- [14] Q. Yang, X.Y. Liu, K. Umetani, N. Kamo, J. Miyake, Partitioning of triphenylalkylphosphonium homologues

- in gel bed-immobilized liposomes; chromatographic measurement of their membrane partition coefficients, *Biochim. Biophys. Acta* 1417(1999)122-130
- [15] N. Kamo, M. Muratsugu, R. Hongoh, Y. Kobatake, Membrane potential of mitochondria measured with an electrode sensitive to tetraphenyl phosphonium and relationship between proton electrochemical potential and phosphorylation potential in steady state, *J. Membr. Biol.* 49 (1979) 105-21
- [16] G.R. Bartlett, Phosphorus assay in column chromatography, *J. Biol. Chem.* 234(1959)466-468
- [17] M.R. Ladisch, *Bioseparations Engineering*, Wiley-Interscience, New York, 2001
- [18] D.H. Freeman, Interaction gel networks. I. Treatment of simple complexation and masking phenomena, *Anal. Chem.* 44(1971)117-120
- [19] C. Huang, J.T. Mason, geometric packing constrains in egg phosphatidylcholine vesicles, *Proc. Nat. Acad. Sci.* 75(1978)308-310
- [20] C. DeLisi, H.W. Hethcote, Chromatographic theory and application to quantitative affinity chromatography, in: I.M. Chaiken (Ed.), *Analytical affinity chromatography*, CRC Press, Boca Raton, 1971, pp.1-63
- [21] T-H. Lee and M-I. Aguilar, Biomembrane chromatography: application to purification and biomolecule-Membrane interactions, in: P.R. Brown and E. Grushka (Eds.),



- Advances in Chromatography vol.41, Marcel Dekker, Inc.,  
New York, 2001, pp.175-201
- [22] R. Aris, N.R. Amundson, Longitudinal mixing of  
diffusion in fixed beds, A. I. Ch. E. Journal 3(1957)  
280-282
- [23] R.A. Weisiger, C.M. Mendel, R.R. Cavalieri, The hepatic  
sinusoid is not well-stirred: Estimation of the degree  
of axial mixing by analysis of lobular concentration  
gradients formed during uptake of thyroxine by the  
perfused-rat-liver, J. Pharm. Sci. 75(1986)233-237
- [24] S. Miyauchi, Y. Sugiyama, Y. Sawada, T. Iga, M. Hanao,  
Conjugative metabolism of 4-methylumbelliferone in the  
rat-liver: verification of the sequestration process  
in multiple indicator dilution experiments, Chem. Pharm.  
Bull. 35(1987)4241-4248
- [25] R.F. Flewelling, W.L. Hubbell, Hydrophobic ion  
interactions with membranes: Thermodynamic analysis of  
tetraphenylphosphonium binding to vesicles, Biophys.  
J. 42(1986)531-540
- [26] P. Smejtek, Permeability of lipophilic ions across  
lipid bilayers, in E.A. Disalvo and S.A. Simon (Eds),  
Permeability and stability of lipid bilayers, CRC Press,  
Boca Raton, 1995, pp.197-240
- [27] A. Ono, S. Miyauchi, M. Demura, T. Asakura, N. Kamo,  
Activation energy for permeation of phosphonium cations  
through phospholipid bilayer membrane, Biochem.

33 (1994) 4312-4318

- [28] S. Miyauchi, A. Ono, M. Yoshimoto, N. Kamo, Tetraphenylphosphonium and its homologues through the planar phospholipid bilayer: concentration-dependence and mutually competitive-inhibition in membrane passive transport, *J. Pharm. Sci.* 82 (1993) 27-31
- [29] J.J. van Deemter, F.J. Znidarweg, A. Klinkenberg, Longitudinal diffusion and resistance to mass transfer as causes of non-ideality in chromatography, *Chem. Eng. Sci.* 5 (1956) 271-289
- [30] E. Grushka, L.R. Snyder, J.H. Knox, Advances in band spreading theories, *J. Chromatogr. Sci.* 13 (1975) 25-37
- [31] Y. Yang, A. Velayudhan, C.M. Ladisch, M.R. Ladisch, Protein chromatography using a continuous stationary phase, *J. Chromatogr.* 598 (1992) 169-180
- [32] K.H. Hamaker, R.M. Ladisch, Intraparticulate flow and plate height effects in liquid chromatography stationary phases, *Separation and Purification Methods* 25 (1996) 47-83
- [33] G. Guiochon, S. Golshan-Shirazi, A.M. Katti, Fundamentals of preparative and non-linear chromatography, Academic Press, Boston, 1994
- [34] K. Miyabe, G. Guiochon, Fundamental interpretation of the peak profiles in: linear reversed-phase liquid chromatography, in P.R. Brown and E. Grushka (Eds.), *Advances in chromatography*, vol 40, Marcel Dekker, New

York, 2000, pp.1-113

- [35] K. Mosbach, O. Ramstrom, The emerging technique of molecular imprinting and its future impact on biotechnology, *Bio-Technology* 14(1996)163-170
- [36] P.T. Vallano, T.T. Remcho, Highly selective separations by capillary electrochromatography: molecular imprint polymer sorbents, *J. Chromatogr. A* 887(2000)125-135
- [37] J. Haginaka and H. Sanbe, Uniform-sized molecularly imprinted polymers for 2-arylpropionic acid derivatives selectively modified with hydrophilic external layer and their applications to direct serum injection analysis, *Anal. Chem.* 72(2000):5206-5210

### Figure Legends

**Figure 1.** The well-mixed zone model, which is proposed here to account for the ILC elution profile. It is assumed that the column is divided into a large number ( $N$ ) of sequential well-mixed compartments (disks). The elution solvent is sequentially moved from the  $i$ -th compartment to the  $(i+1)$ -th compartment at a flow rate of  $Q$ .  $V_0$  is a volume of the mobile phase within the column, and  $V_0/N$  is the volume of the mobile phase of the compartment.

**Figure 2.** Elution patterns of the phosphonium cation  $\text{TPP}^+$  from an ILC column at various flow rates. The amount of immobilized liposomes was  $35.6 \mu\text{mol}$  phospholipid per 5 cm column length. The flow rate ranged from 0.3 to 1.5 ml/min.

**Figure 3.** The relationship between mean resident time and the reciprocal of the flow rate. The mean resident time was calculated from Eq. 1, and the flow rate ranged from 0.3 to 1.5 ml/min. The amount of immobilized liposomes was  $35.6 \mu\text{mol}$  of phospholipid. The straight lines passing through the origin were calculated by linear regression analysis.

**Figure 4.** Membrane partition coefficients ( $K_{LM}$ ) under various conditions. The membrane partition coefficients were calculated from Eq. 5. The  $K_{LM}$  values remain unchanged under

various conditions and Eq.13 holds for the ILC column. Panels A), B) and C) represent  $K_{LM}$  obtained for various flow rates, injected quantities and gel bed volume, respectively.

**Figure 5.** The relationship between variance and the reciprocal of the flow rate. The variance of the elution pattern was calculated from Eq. 2, and the flow rate ranged from 0.3 to 1.5 ml/min. The amount of immobilized liposome was 28.5  $\mu$ mol of phospholipid. The lines represent fitted curves using Eq. 25 and an iterative nonlinear least-squares method.

**Figure 6.** The effect of injection volume on the number of well-mixed zones (N). Using a nonlinear iterative least-square method, the relationship between variance and the reciprocal of the flow rate as in Fig. 5 was fitted to Eq.25, from which the values of N were obtained.  $\circ$ , TPBP<sup>+</sup>;  $\bullet$ , TPP<sup>+</sup>.

**Figure 7.** The effect of injection volume on the estimated rate constants  $k_1$  and  $k_{-1}$ . The experimental conditions were the same as those for Fig. 6. The closed and open symbols represent the rate constants  $k_1$  and  $k_{-1}$ , respectively and the squares and circles represent the values of TPBP<sup>+</sup> and TPP<sup>+</sup>, respectively.

**Figure 8.** The membrane partition coefficient (A), and association and dissociation rate constants (B) of various phosphonium cations. The values of  $K_{LM}$ ,  $k_1$  and  $k_{-1}$  were calculated by fitting the data depicted in Figs. 4 and 6 to Eq. 24 and 25, respectively. The abscissa,  $n$ , represents the number of methylenes in the alkyl chain. The open (○) and closed (●) circles represent  $k_1$  and  $k_{-1}$ , respectively.

Figure 1

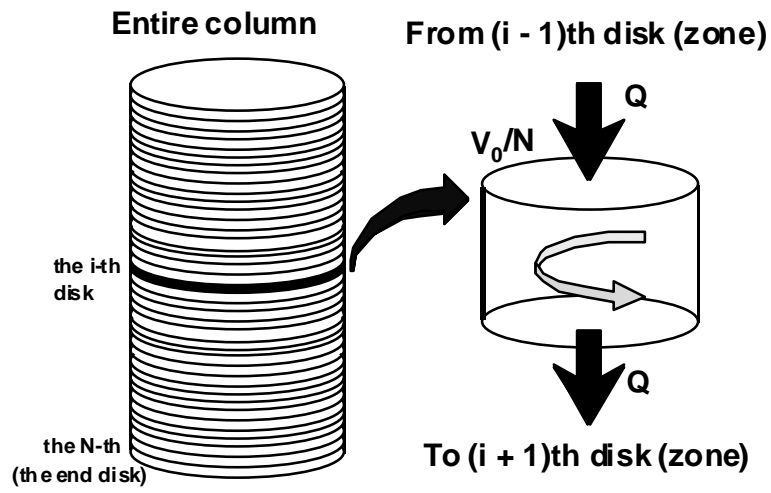


Figure 2

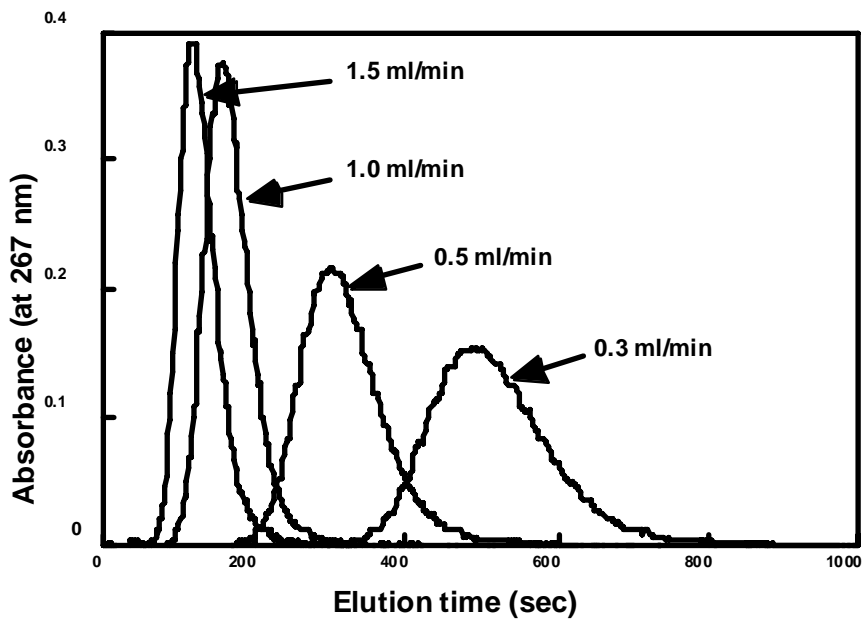




Figure 3

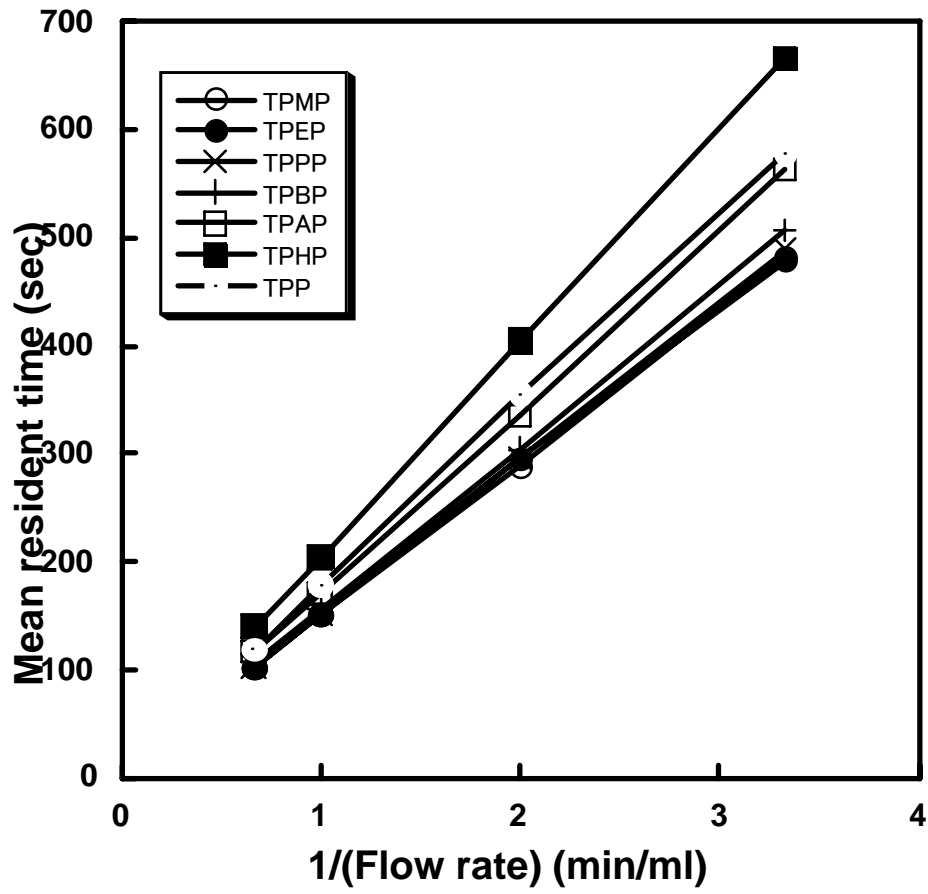


Figure 4

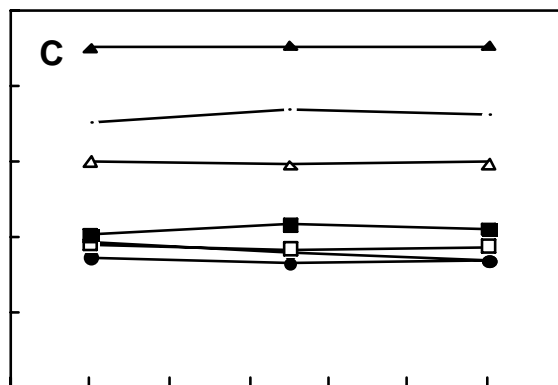
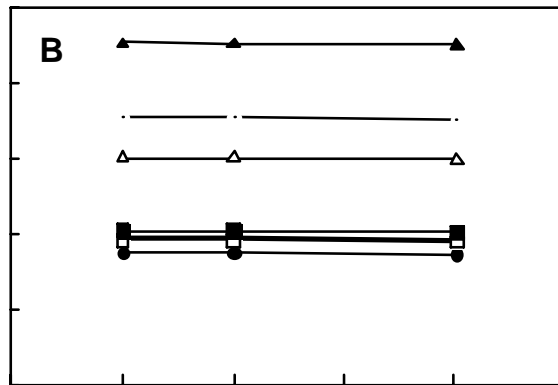
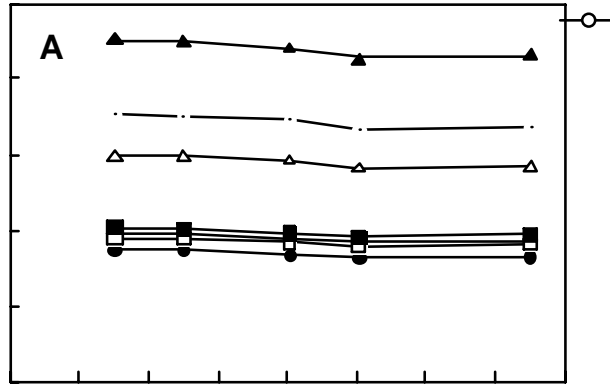


Figure 5

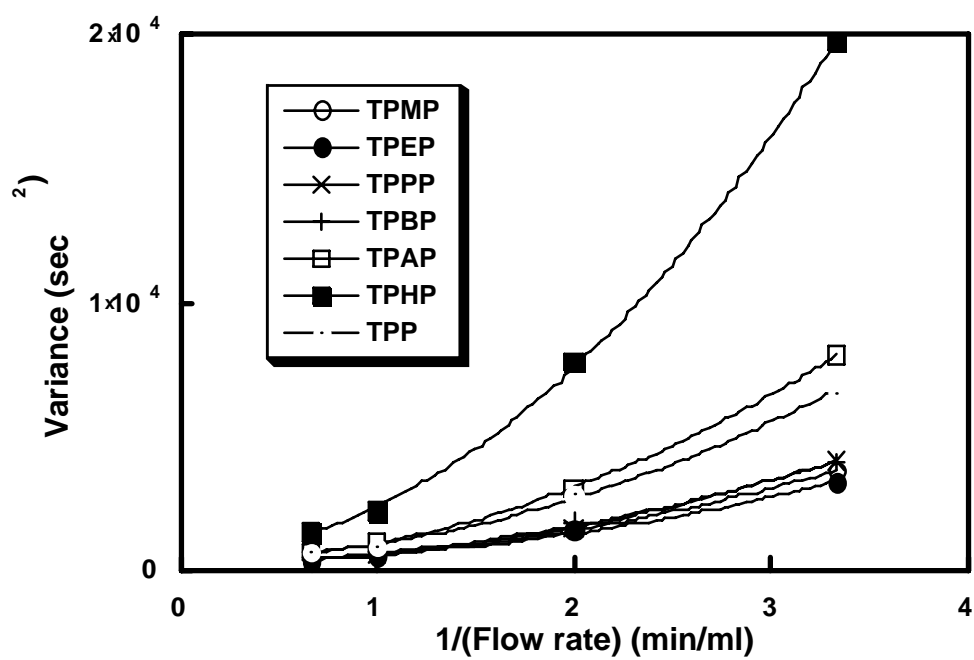


Figure 6

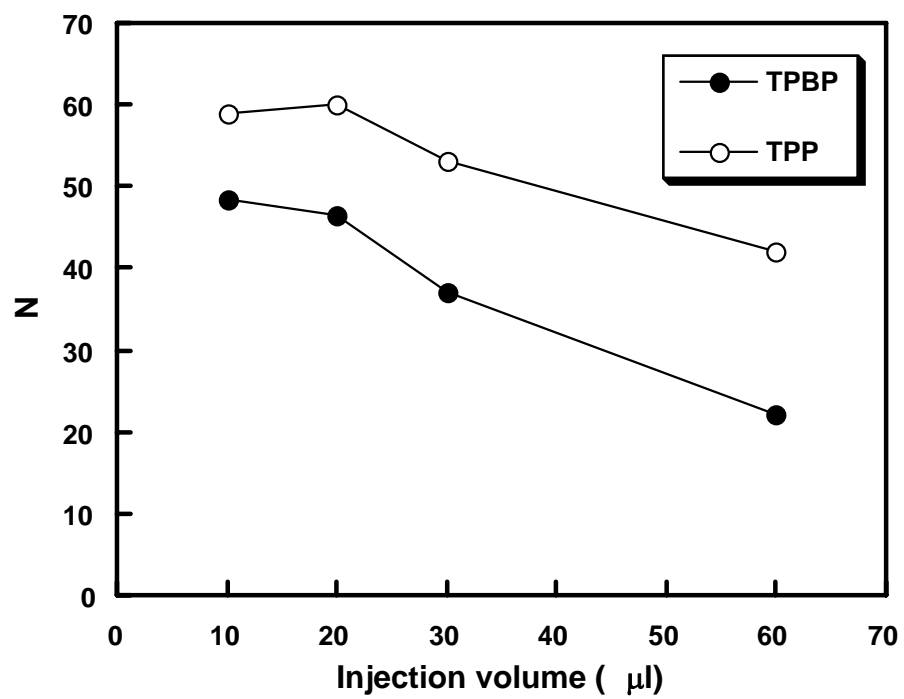


Figure 7

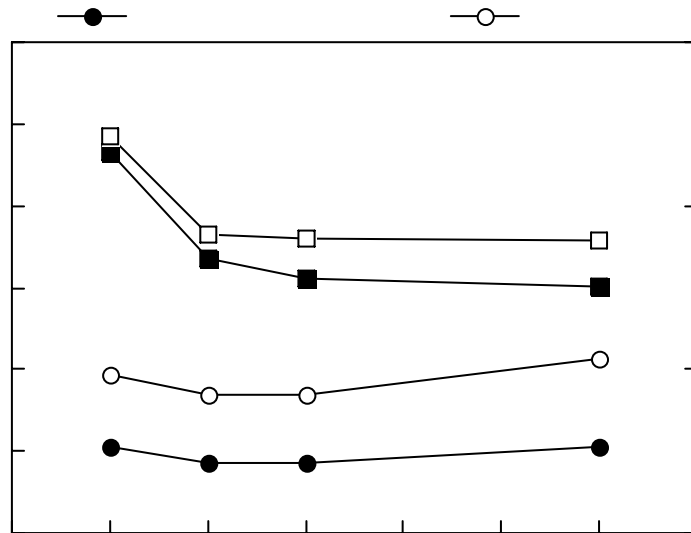


Figure 8

